

## Non-Crossing Frameworks with Non-Crossing Reciprocals\*

David Orden,<sup>1</sup> Günter Rote,<sup>2</sup> Francisco Santos,<sup>1</sup> Brigitte Servatius,<sup>3</sup>  
Herman Servatius,<sup>3</sup> and Walter Whiteley<sup>4</sup>

<sup>1</sup>Departamento de Matemáticas, Estadística y Computación, Universidad de Cantabria,  
E-39005 Santander, Spain  
{ordend,fsantos}@unican.es

<sup>2</sup>Institut für Informatik, Freie Universität Berlin,  
Takustraße 9, D-14195 Berlin, Germany  
rote@inf.fu-berlin.de

<sup>3</sup>Department of Mathematical Sciences, Worcester Polytechnic Institute,  
Worcester, MA 01609, USA  
{bservat,hservat}@wpi.edu

<sup>4</sup>Department of Mathematics and Statistics, York University,  
Toronto, Ontario, Canada M3J 1P3  
whiteley@mathstat.yorku.ca

**Abstract.** We study non-crossing frameworks in the plane for which the classical reciprocal on the dual graph is also non-crossing. We give a complete description of the self-stresses on non-crossing frameworks  $G$  whose reciprocals are non-crossing, in terms of: the types of faces (only pseudo-triangles and pseudo-quadrangles are allowed); the sign patterns in the stress on  $G$ ; and a geometric condition on the stress vectors at some of the vertices.

As in other recent papers where the interplay of non-crossingness and rigidity of straight-line plane graphs is studied, *pseudo-triangulations* show up as objects of special interest. For example, it is known that all planar Laman circuits can be embedded as a pseudo-triangulation with one non-pointed vertex. We show that for such pseudo-triangulation embeddings of planar Laman circuits which are sufficiently generic, the reciprocal is non-crossing and again a pseudo-triangulation embedding of a planar Laman circuit. For a singular (non-generic) pseudo-triangulation embedding of a planar Laman circuit, the reciprocal is still non-crossing and a pseudo-triangulation, but its underlying graph may not be a Laman circuit. Moreover, all the pseudo-triangulations which admit a non-crossing re-

---

\* The first and third authors were supported by Grant BFM2001-1153, Spanish Ministry of Science and Technology, the second author was partly supported by the Deutsche Forschungsgemeinschaft (DFG) under Grant RO 2338/2-1, and the last author was supported by grants from NSERC (Canada) and NIH (US).



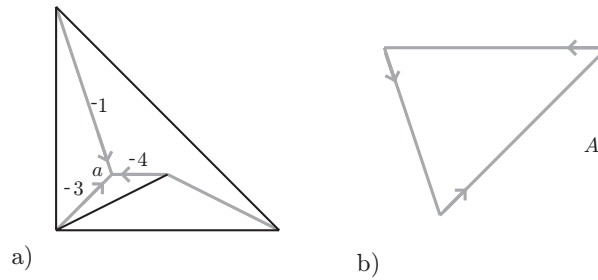


**Fig. 2.** The equilibrium forces at vertex  $a$  produce a polygon of forces  $A$ .

equilibrium forces in a planar framework generates a reciprocal framework, unique up to translation, and each reciprocal prescribes a set of forces in equilibrium.

Reciprocal figures were first developed in the 19th century as a graphical technique to calculate when external static forces on a plane framework reach an equilibrium at all the vertices with resolving tensions and compressions in the members [16], [8], and were the basis for *graphical statics* in civil engineering. A famous application: this technique was used to check the Eiffel tower prior to construction [5], [9].

Classically, there are two graphic forms for the reciprocal. In the engineering work adapted to graphical techniques at the drafting table by the mathematician and engineer Cremona [8], the edges of the reciprocal are drawn parallel to the edges of the original. We use this “Cremona” form of the reciprocal in most of our proofs.

In the original work of Maxwell, the edges of the reciprocal are drawn perpendicular to the edges of the original framework. This form is adapted to viewing the framework on a planar graph as a projection of a spatial polyhedron and the reciprocal as a drawing of the dual polyhedron. The surprise is that this image captures an exact correspondence: a framework with a planar graph has a self-stress if and only if it is the exact projection of a spatial, possibly self-intersecting, spherical polyhedron, see Fig. 4, with non-zero dihedral angles directly corresponding to the non-zero forces in the self-stress of the projection [16], [8], [26], [6], [25]. Moreover, the reciprocal diagram is the projection of a very specific spatial polar of the original projected polyhedron. We return to an application of this correspondence with spatial polyhedra in Section 4. This spatial

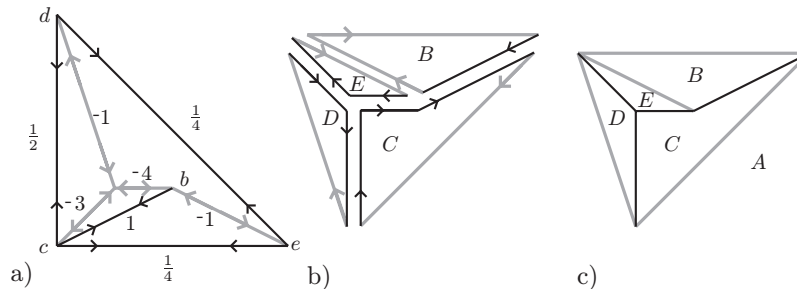


**Fig. 3.** Assembling the reciprocal.

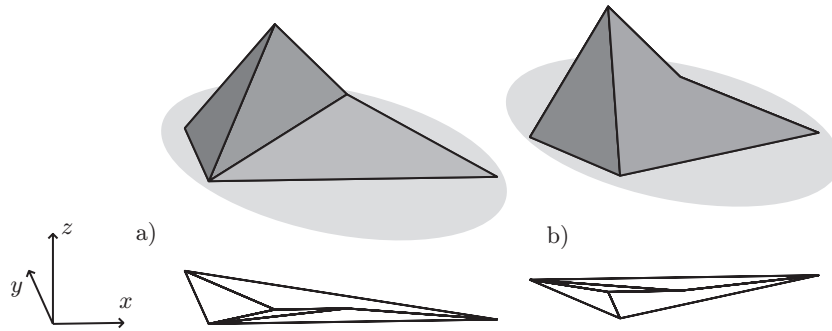


Fig. 4. The lift of the frameworks of Fig. 3.

polarity also reinforces the reciprocal relationship for plane frameworks, since either framework can be viewed as the original and the other viewed as its reciprocal. It is not difficult to check that given one presentation of the reciprocal, we can simply turn it  $90^\circ$  to create the other presentation.

Reciprocal diagrams were rediscovered as a technique to check whether a given plane drawing is the exact projection of a spatial polyhedron or a polyhedral surface [12], [13]. Here the reciprocal diagram is also called the “gradient diagram”, since the vertices of the reciprocal can be located as the points of intersection of normals to the faces of the original polyhedron, with the projection plane, with all normals drawn from a fixed center above the plane. These points are the gradients representing the slopes of the faces. This gradient diagram is a Maxwell reciprocal with reciprocal edges perpendicular to the edges of the original [6]. A related construction, starting with points on the paraboloid  $x^2 + y^2 - z = 0$  and their convex hull, creates the Delaunay triangulation of the projected points, with the Voronoi cells as a (Maxwell) reciprocal diagram [2].

## 1.2. Our Contribution

In this paper we connect planarity with the theory of reciprocals: we investigate when both the original graph drawing, or framework, and the reciprocal diagram are crossing free. We show in Section 2 that interior faces of both drawings must be pseudo-triangles or pseudo-quadrangles, the outer boundary must be convex and the self-stress generating the reciprocal must have a specific type of sign pattern. With one additional geometric condition on the self-stress at non-pointed vertices, these conditions become both necessary and sufficient for creating a reciprocal pair of non-crossing frameworks. We address separately the interesting cases in which the framework is a Laman circuit (an edge-minimal graph that can sustain a self-stress in a generic embedding), a pseudo-triangulation or has a unique non-pointed vertex.

Of particular interest are Laman circuits embedded as pseudo-triangulations, because they possess a unique non-pointed vertex and hence combine all three properties just mentioned, as shown in previous work [11]. In Section 3 we show that they produce non-crossing reciprocals. For sufficiently generic embeddings the reciprocals are also Laman

circuits realized as pseudo-triangulations with one non-pointed vertex, so the pairing is a complete reciprocity. This result extends to Laman circuits realized as non-generic pseudo-triangulations, with self-stresses that are zero on some edges, again showing that the reciprocal is a pseudo-triangulation (with several non-pointed vertices, in general). Moreover, any pseudo-triangulation with a self-stress and a non-crossing reciprocal occurs in a pair with a possibly singular pseudo-triangulation on a Laman circuit.

Section 4 studies the characteristic features of the lifts of such non-crossing reciprocal pairs. Essentially, they look like negatively curved surfaces with a unique singularity at the vertex whose reciprocal is the outer face. In particular, that vertex is the unique local maximum of the surface, the outer face is the unique local minimum and there are no (horizontal) saddle-points.

Section 5 lists some open problems.

### 1.3. Preliminaries—Frameworks

An  $n$ -dimensional framework  $(G, \rho)$  is a graph  $G = G(V, E)$  with vertex set  $V$  and edge set  $E$ , together with an embedding  $\rho: V \rightarrow \mathbb{R}^n$ , and we write  $\rho(i) = \mathbf{p}_i$ . We only consider plane frameworks, i.e.  $n = 2$ . The edges of  $(G, \rho)$  are regarded as abstract length constraints on the motions of the points  $\mathbf{p}_i$ . The edges are drawn as straight line segments, which may, of course, cross. In the absence of any edge crossing, we say that the framework is *non-crossing*.

Infinitesimally, length constraints form a linear system, with an equation for each edge  $\{i, j\} \in E$ ,

$$(\mathbf{p}'_i - \mathbf{p}'_j) \cdot (\mathbf{p}_i - \mathbf{p}_j) = 0.$$

This system of equations in the unknowns  $\mathbf{p}'_i$  has a coefficient matrix of size  $|E| \times 2|V|$ ; we call it the *rigidity matrix* of the framework. The framework is called *infinitesimally rigid* if its rigidity matrix has rank  $2|V| - 3$ . When  $G$  is the complete graph the rigidity matrix has size  $\binom{|V|}{2} \times 2|V|$  and rank  $2|V| - 3$  (unless all the vertices lie on a single line). The matroid on the rows of the rigidity matrix of the complete graph, called the *rigidity matroid* [10], [27] of the point set  $\rho(V)$ , is interesting because its spanning subsets are precisely the infinitesimally rigid frameworks with vertex set  $\rho(V)$ .

The rigidity matroid is the same for all generic choices of vertex positions, and is called the *generic rigidity matroid*. Its spanning subgraphs are called *generically rigid graphs* and the minimal ones, bases of the matroid, are called *isostatic* or *Laman graphs*, and they are characterized by the *Laman condition*:  $G = (V, E)$  is isostatic if and only if  $|E| = 2|V| - 3$  and every subset of  $k \geq 2$  vertices spans at most  $2k - 3$  edges of  $E$  [15]. Generically rigid graphs are those containing a spanning *Laman subgraph*. Every circuit of the generic rigidity matroid which spans  $k$  vertices must consist of exactly  $2k - 2$  edges, and is called a *Laman circuit*.

In a dual analysis of this matrix, a stress on a framework  $(G, \rho)$  is an assignment of scalars  $\omega: E \rightarrow \mathbb{R}$ . A stress is *resolvable* or a *self-stress* of the framework if the weighted sum of the displacement vectors corresponding to each vertex cycle (the star

of each vertex) is zero;

$$\sum_{j|(i,j) \in E} \omega_{ij}(\mathbf{p}_i - \mathbf{p}_j) = \mathbf{0} \quad \text{for all } i \in V.$$

That is to say, the self-stresses form the cokernel of the rigidity matrix. If the graph is generically rigid and the embedding is generic, then the dimension of the space of self-stresses is  $|E| - (2|V| - 3)$ . In particular, a Laman circuit in a generic embedding has a unique (up to a scalar multiple) self-stress, which is non-zero on every edge.

#### 1.4. Preliminaries—Reciprocal Diagrams

A graph  $G$  is planar if it can be (topologically) embedded in the plane, with distinct points representing the vertices and the edges corresponding to Jordan arcs, such that two Jordan arcs may only intersect in a common endpoint. A topologically embedded planar graph is called a *plane graph*. The embedding determines for each face the sequences of edges that lie on the boundary (the *face cycles*) and the sequences of edges that lie around each vertex (the *vertex cycles*). From a plane graph  $G$  we obtain the geometric dual  $G^*$  by interchanging the role of vertices and faces. If  $G$  is 3-connected and planar, then face cycles as well as the vertex cycles are uniquely determined by  $G$ , and the  $G^*$  is independent of the embedding of  $G$ . If the connectivity of  $G$  is less than 3, then  $G$  might have several essentially different embeddings in the plane, each with its own collection of face cycles and vertex cycles, yielding non-isomorphic dual graphs. If  $G$  is at least 2-connected, the face cycles are minimal closed paths and the faces are topological disks, while the vertex cycles are actually cocycles (minimal cutsets), so the corresponding dual edges bound a face in the dual.

Every plane graph gives rise to a framework by leaving the positions of the points fixed and replacing the Jordan arcs representing the edges by straight line segments, which of course may cross. Given a plane graph  $G$  and a framework  $(G, \rho)$  on  $G$ , a second framework on the plane dual graph  $G^*$  is *reciprocal* to the first if corresponding edges are parallel.

Even if the framework  $(G, \rho)$  is already non-crossing, one may choose to use a different plane embedding of  $G$  for computing the reciprocal. However, in this paper we only consider the case where  $(G, \rho)$  is non-crossing and the embedding of  $G$  is given by  $\rho$ .

We say that a reciprocal  $(G^*, \rho^*)$  is a *non-crossing reciprocal* of  $(G, \rho)$  if  $(G^*, \rho^*)$  is non-crossing *and* its embedding is dual to the embedding of  $(G, \rho)$ . Our goal is to characterize pairs of simultaneously non-crossing reciprocal diagrams. As a first (counter-)example, Fig. 1 shows a non-crossing framework with a crossing reciprocal. We shall see that this is actually the “typical situation”.

Observe that, in principle, if a non-crossing graph has a non-crossing reciprocal, the reciprocity may preserve or reverse the orientation. That is, vertex cycles of  $(G, \rho)$  may in become face cycles in  $(G^*, \rho^*)$  in the same or the opposite directions. We will prove that only the orientation-reversing situation occurs.

Reciprocity of frameworks is very closely related to self-stresses. We offer a simple representation of the Cremona reciprocal for a plane graph  $G$ . We denote the set of all

directed edges of  $G$  and their inverses by  $E^\pm$ . The inverse of an edge  $e$  is denoted by  $\bar{e}$ , with  $\bar{\bar{e}} = e$ . Let  $g: E^\pm \rightarrow \mathbb{R}^2$  be an assignment of unit vectors to the edges of  $G$  with  $g(\bar{e}) = -g(e)$ ,  $|g(e)| = 1$ . For simplicity we write  $g(e) = \mathbf{e}$ . Suppose we have two scalar functions  $\alpha: E \rightarrow \mathbb{R}$  and  $\beta: E \rightarrow \mathbb{R}$  with compatibility conditions,

$$\sum_{e \in C} \alpha_e \mathbf{e} = \mathbf{0}, \quad \sum_{e \in C'} \beta_e \mathbf{e} = \mathbf{0} \tag{1}$$

for each face cycle  $C$  and each vertex cycle  $C'$ .

Since the face cycles corresponding to a plane graph embedding generate the entire cycle space of the graph, the cycle conditions in (1) are sufficient to guarantee that the displacement vectors  $\alpha_e \mathbf{e}$  are consistent over the entire framework. Hence, they are the displacements or edge vectors of a framework  $(G, \rho)$  on the graph  $G$ . Similarly, the vectors  $\beta_e \mathbf{e}$  correspond to edge displacements of a framework  $(G^*, \rho^*)$  on the dual graph  $G^*$ . In particular, the two frameworks are reciprocal to each other. However, now the face equalities for  $G^*$  can be read as equilibrium conditions for the vertices of  $(G, \rho)$  and vice versa. Hence, if all  $\alpha_e \neq 0$  then the values  $\beta_e/\alpha_e$  are a self-stress on the framework  $(G, \rho)$ . Similarly, if  $\beta_e \neq 0$  then the values  $\alpha_e/\beta_e$  are a self-stress on the framework  $(G^*, \rho^*)$ .

This argument can be reversed, so a unique reciprocal framework can be constructed starting with a self-stress on  $(G, \rho)$  [6], [7]. It follows that the self-stresses of a connected framework  $G$  are in one-to-one correspondence with the reciprocals of  $G$  (up to translation). Multiplication of the self-stress by a constant corresponds to scaling the reciprocal. In particular, changing the sign of a self-stress will rotate the reciprocal by  $180^\circ$ . Thus, if the framework  $G$  has a unique self-stress (up to scalar multiplication), we can speak of *the* reciprocal framework if we are not interested in the scale.

Maxwell proved that the projection of a spherical polyhedron from 3-space gives a plane diagram of segments and points which forms a stressed bar and joint framework. This proof, and related constructions, were built upon an analysis of reciprocal diagrams [16]. Crapo and Whiteley [7], [26] gave new proofs for Maxwell’s theorem as well as its converse for planar graphs. See [6] and [7] for more details on the full vector spaces of self-stresses, reciprocals and spatial liftings of a plane drawing.

### 1.5. Preliminaries—Pseudo-Triangulations

Given a non-crossing embedding  $\rho: V \rightarrow \mathbb{R}^2$  of a planar graph, we say that the vertex  $i$  is *pointed* if all adjacent points  $\mathbf{p}_j$  lie strictly on one side of some line through  $\mathbf{p}_i$ . In this case some pair of consecutive edges in the counterclockwise order around  $i$  spans a *reflex angle* or *big angle*, i.e. an angle larger than  $180^\circ$ . A face of the non-crossing framework is a *pseudo-triangle* if it is a simple planar polygon with exactly three convex vertices (called *corners*). Interior angles at the corners of a pseudo-triangle are small (smaller than  $180^\circ$ ), all other interior angles are big. A *pseudo-triangulation* is an embedding whose interior faces are pseudo-triangles and the complement of the outer face is a convex polygon. Figure 5 shows an example. In a *pointed pseudo-triangulation* all the vertices are pointed. Pseudo-triangulations have arisen as important objects connecting rigidity and planarity of geometric graphs. For example, pointed pseudo-triangulations were an important tool

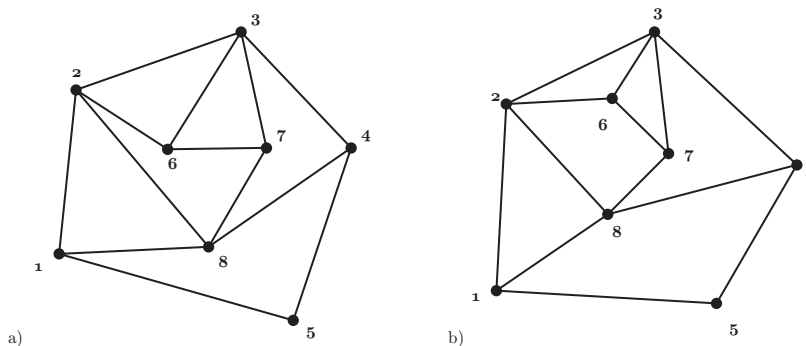


**Fig. 5.** (a) A pointed pseudo-triangulation. (b) A different embedding of the same graph which is not a pseudo-triangulation.

in straightening the carpenter's rule [23]. In this paper we need to extend the concept of pseudo-triangulation to that of *pseudo-quadrangulation*. A *pseudo-quadrangle* is a simple polygon with four convex vertices (corners) and a pseudo-quadrangulation is a decomposition of a convex polygon into pseudo-triangles and pseudo-quadrangles.

**Lemma 1.** *Let  $T$  be a pseudo-quadrangulation with  $e$  edges,  $x$  non-pointed vertices,  $y$  pointed vertices,  $t$  pseudo-triangles and  $q$  pseudo-quadrangles. Then*

$$2e = t + 3y + 4x - 4.$$

*Proof.* The pseudo-quadrangulation has  $3t + 4q$  convex angles and  $y$  reflex angles (one at each pointed vertex). Since the total number of angles is  $2e$ , we get  $2e = 3t + 4q + y$ . Euler's formula gives  $e = x + y + t + q - 1$ . Eliminating  $q$  gives the desired equation.  $\square$

In the case of pseudo-triangulations ( $q = 0$ ) this lemma is well known and usually stated under the equivalent form  $e = (2n - 3) + x$ , where  $n = x + y$  is the total number of vertices [11], [17]. Since every pseudo-triangulation is infinitesimally rigid [18], this formula says that:

**Lemma 2.** *The dimension  $d$  of the space of self-stresses of a pseudo-triangulation equals its number of non-pointed vertices, that is,  $d = e - (2n - 3)$ .*

Moreover, it is easy to prove that every non-crossing framework can be extended, by adding edges, to a pseudo-triangulation with exactly the same number of non-pointed vertices [20, Theorem 6]. The next lemma follows.

**Lemma 3.** *The dimension of the space of self-stresses of a non-crossing framework is at most its number of non-pointed vertices.*



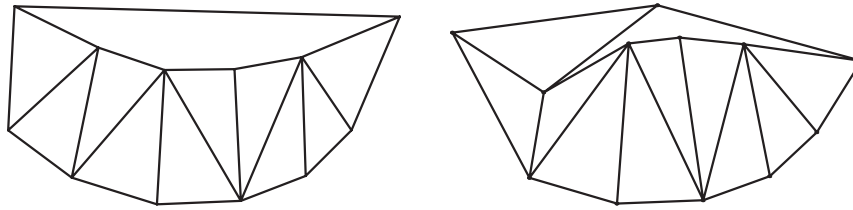


**Fig. 6.** A Laman circuit and one of its embeddings as a pseudo-triangulation with exactly one non-pointed vertex.

A graph is planar and generically rigid if and only if it can be embedded as a pseudo-triangulation [17]. It is planar and isostatic if and only if it can be embedded as a pointed pseudo-triangulation [11]. These embedding results have extensions for Laman circuits. A *pseudo-triangulation circuit* is a planar Laman circuit embedded as a pseudo-triangulation. A pseudo-triangulation circuit has a single non-pointed vertex, by Lemma 2.

See Fig. 6 for an example of a Laman circuit (a Hamiltonian polygon triangulation with an added edge between its two vertices of degree 2) and one of its embeddings as a pseudo-triangulation with exactly one non-pointed vertex. A basic starting point for our analysis is the following result from [11].

**Theorem 1** [11]. *Every topologically embedded planar Laman circuit with a given outer face and a specified vertex  $v$  that does not lie on the outer face has a realization as a pseudo-triangulation where  $v$  is the single non-pointed vertex.*

These pseudo-triangulation circuits are the main focus of Section 3.

### 1.6. Geometric versus Singular Circuits

Given a planar Laman circuit  $G$ , there is a range of realizations as frameworks in the plane, all of which are dependent, i.e. have a non-trivial space of self-stresses. For an open dense subset of these realizations, containing the generic realizations, the unique (up to scalar multiplication) self-stress is non-zero on all edges. For realizations in this set we say the graph is embedded as a *geometric circuit*. Figure 7(a) depicts an example.

The remaining *singular realizations* are frameworks on which either the one-dimensional space of self-stresses vanishes on some subset of edges, as in Fig. 7(b) in which the dashed edges are unstressed, or for which the space of self-stresses has higher dimension, in which case it is generated by self-stresses which vanish on some of the edges. See Fig. 7(c). The singular self-stresses of Fig. 7(b) will cause some complications in the reciprocal diagrams: the original edge effectively disappears as a division between faces and the corresponding reciprocal edge has zero length, fusing the reciprocal pair of vertices into one. We can actually track such singular frameworks  $\rho$  on the graph as those whose vertex coordinates satisfy at least one of a set of  $e$  polynomials,  $C_{i,j}(\rho)$ ,

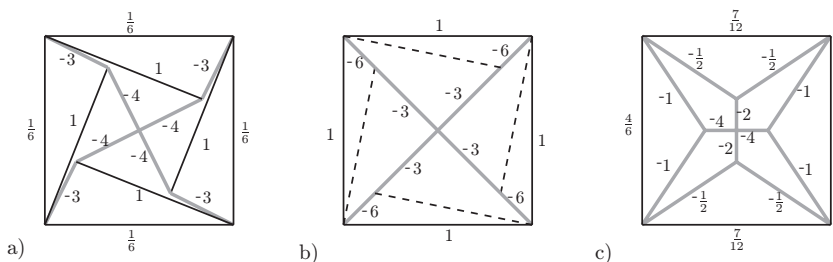


**Fig. 7.** A geometric circuit (a), a singular realization with dropped edges (b) and a singular realization with additional self-stresses (c).

representing the pure conditions for the independence of the subgraphs with the edge  $i, j$  removed [25]. In general, the coefficients of the unique self-stress of a geometric circuit on the original graph can be written using these polynomials as coefficients. An edge has a zero coefficient in the self-stress if and only if the corresponding polynomial is zero.

However, all realizations as pseudo-triangulations are not guaranteed to be geometrical circuits, since they need not be generic embeddings. In the pseudo-triangulation of Fig. 8, the edge  $CF$  does not participate in the self-stress when the edges  $AD$ ,  $BF$  and  $CE$  are concurrent, for projective geometric reasons. By Lemma 2, all pseudo-triangulation realizations of this graph will have a one-dimensional space of self-stresses, but the stress may be singular.

## 2. Simultaneously Non-Crossing Reciprocals

Assume we are given a non-crossing framework  $(G, \rho)$ , and a particular everywhere non-zero self-stress from which to construct the reciprocal. The goal of this section is to determine when the framework and its reciprocal are both non-crossing. Our main result, Theorem 4, is that for this to happen the framework must be a pseudo-quadrangulation and the signs of the self-stress must satisfy certain necessary (and almost sufficient) conditions to make the reciprocal non-crossing.

In order to include all degeneracies that arise in non-crossing reciprocal pairs, we do not assume our framework to be in general position. In particular, angles of exactly  $\pi$

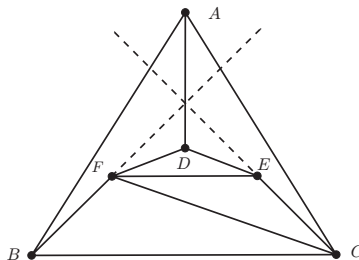


**Fig. 8.** A Laman circuit with a singular self-stress.

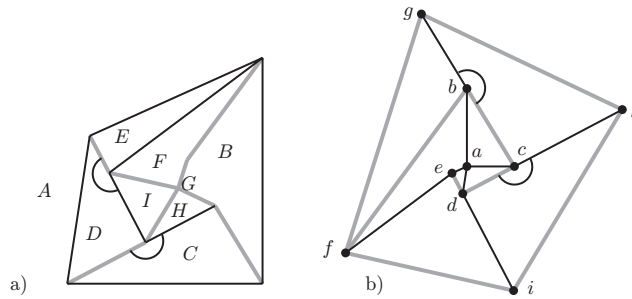


**Fig. 9.** We can have flat angles on both sides of a non-crossing reciprocal pair.

(to be called *flat angles*) can arise and, by convention, we treat them as convex (“small”) angles. In particular, a vertex having one flat angle is necessarily non-pointed, and the face incident to it cannot be a pseudo-triangle, see Figs. 9 and 10. We do not allow degeneracies in which the angle is zero, as these produce overlapping, hence crossing, edges. Also, vertices with two flat angles have degree two and produce a double edge in the reciprocal, so we do not allow them in our frameworks.

Recall that for a reciprocal non-crossing pair  $(G, \rho)$  and  $(G^*, \rho^*)$ , the face cycles in  $(G, \rho)$  must form the vertex cycles in  $(G^*, \rho^*)$ . In principle, the face cycles could become vertex cycles with either the same or the opposite orientation, but the orientation must be globally consistent: either all the cycles keep the orientation or all of them reverse it. Special care needs to be taken with the exterior face, for which the orientation must be considered “from outside”: if the orientation is chosen counterclockwise for interior faces, it will be clockwise for the outer face.

2.1. *The Reciprocal of a Single Face*

We concentrate on a single face of our framework  $G$ . That is to say, let  $F$  be a simple polygon in the plane. If  $F$  has  $k$  convex vertices we say it is a pseudo- $k$ -gon.

Given a vertex  $v$  of  $F$ , we call the *reduced internal angle of  $F$  at  $v$*  the internal angle itself if  $v$  is a convex vertex (corner) of  $F$ , and the angle minus  $\pi$  if it is not. In other

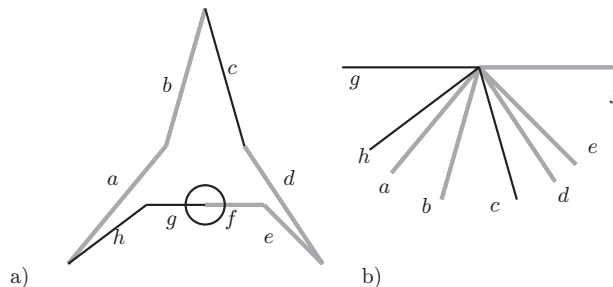


**Fig. 10.** Locally, the reciprocal of a pseudo-quadrangle with a flat vertex as a corner is a flat vertex.

words, we are “reducing” all angles to lie in the range  $0 < \theta \leq \pi$ . Our first result generalizes the elementary fact that the total internal angle of a  $k$ -gon is  $(k - 2)\pi$ .

**Lemma 4.** *The sum of the reduced internal angles of a pseudo- $k$ -gon is  $(k - 2)\pi$ .*

*Proof.* If the polygon has  $n$  vertices, the sum of (standard) internal angles is  $(n - 2)\pi$ , and the reduction process subtracts  $(n - k)\pi$ .  $\square$

Now let signs be given to the edges of  $F$ , intended to represent the signs of a self-stress in the framework of which  $F$  is a face. In this section we assume no sign is zero, which is not really a loss of generality: if a self-stress is zero on some edges then it is a self-stress on the subframework on which it is not zero and the reciprocal depends only on that subframework.

In the reciprocal framework,  $F$  corresponds to a vertex to which the reciprocal edges are incident. To draw the reciprocal edges we use the following rule: Edges are oriented counterclockwise along the face boundary to form the boundary polygon. Edges with positive stress will produce reciprocal edges pointing in the same direction as the original, and edges with negative stress will produce reciprocal edges pointing in the opposite direction at the vertex dual to  $F$ . These conventions are no loss of generality; the opposite choice would produce a reciprocal rotated by  $\pi$ . The length of a reciprocal edge is the length of the original edge scaled by the absolute value of the stress on that edge.

What are the conditions for the reciprocal to be “locally” non-crossing? The reciprocal edges must appear around the reciprocal vertex of  $F$  in the same cyclic order as they appear in  $F$ . That is to say, if  $e_1$  and  $e_2$  are two consecutive edges of  $F$  and  $e_1^*$  and  $e_2^*$  are the reciprocal edges, we want the angle from  $e_1^*$  to  $e_2^*$  in the reciprocal to contain no other edge (the reciprocal angle is oriented the same as the angle between  $e_1$  and  $e_2$  along  $F$  in the orientation-preserving case and opposite otherwise). A necessary and sufficient condition for this to happen is that the angles between reciprocals of consecutive edges of  $F$  add up to  $2\pi$ . We are now going to translate this into a condition on the signs of edges.

We first look at the orientation-reversing case. Let  $e_1$  and  $e_2$  be two consecutive edges of  $F$  with common vertex  $v$ . We say that the angle at  $v$  has a *face-proper* signature (or that the angle of  $F$  at  $v$  is face-proper, for short) if either  $v$  is a corner of  $F$  and the signs of  $e_1$  and  $e_2$  are opposite, or  $v$  is not a corner and the two signs are equal. When the signature is not face-proper (a corner with no sign change or a reflex-angle with sign change) we call it *vertex-proper*. The reason for this terminology is that when rotating a ray around a vertex, the fastest (“proper”) way of going from an edge to the next one is to keep the direction of the ray for a big angle and to change to the opposite ray (“changing signs”) when the angle is small. Analogously, when sliding a tangent ray around a polygon, we should change to the opposite direction at corners.

The key fact now is that the reciprocal angle (measured clockwise) of a given vertex  $v$  of  $F$  equals the reduced internal angle at  $v$  if the signature is face-proper, and it equals the reduced internal angle plus  $\pi$  if it is vertex-proper. Hence:

**Lemma 5.** *The sum of angles (all measured clockwise) between reciprocals of consecutive edges of  $F$  equals the total reduced internal angles of  $F$  plus  $\pi$  times the number*

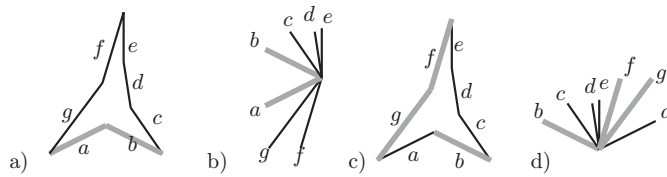


**Fig. 11.** (a) A pseudo-triangle with one vertex-proper angle, at the corner between  $e$  and  $f$ , and (b) its reciprocal vertex. (c) A pseudo-triangle with one vertex-proper angle between  $a$  and  $b$ , not at a corner, and (d) its reciprocal vertex. Stress signs are indicated by line weights.

of vertex-proper angles. In particular, in order for  $F$  to produce a planar reciprocal with the orientation reversed,  $F$  must be either a pseudo-quadrangle with no vertex-proper angle, or a pseudo-triangle with only one vertex-proper angle. If there is a flat angle  $\pi$ , it must occur in a pseudo-quadrangle with a sign change at all corners (one of which is the flat angle).

*Proof.* The two cases described are the only ways of getting  $(k - 2)\pi + s\pi = 2\pi$ , where  $k$  is the number of corners (and hence  $(k - 2)\pi$  is the reduced internal angle of  $F$ ) and  $s$  is the number of vertex-proper angles.

If one of the convex angles is flat, then there must be four convex angles to achieve a non-crossing polygon. Then  $F$  is a pseudo-quadrangle with a sign change at each of the corners.  $\square$

Figure 11 and the left half of Fig. 12 illustrate the cases permitted by Lemma 5. Thick and thin lines represent the two different signs. The case of a pseudo-triangle produces two different pictures, depending on whether the vertex-proper angle happens at a corner (Fig. 11(a)) of the pseudo-triangle or at a reflex vertex (Fig. 11(c)). Parts (b) and (d) show the reciprocal vertex with its incident edges.

The conditions for the orientation-preserving case are now easy to derive, and are illustrated in Fig. 12(c), (d).

**Lemma 6.** *Let  $n$  be the number of vertices in  $F$ . The sum of angles (all measured counterclockwise) between reciprocals of consecutive edges of  $F$  equals  $2n\pi$  minus the total reduced internal angle of  $F$  and minus  $\pi$  times the number of vertex-proper sign changes. In particular, in order for  $F$  to produce a planar reciprocal with the same orientation,  $F$  must be a strictly convex polygon and all edges must have the same sign.*

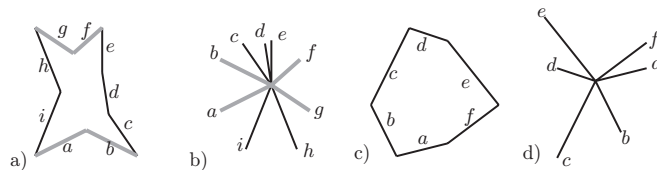


**Fig. 12.** A pseudo-quadrangle with all angles face-proper (a) and a convex face with no sign changes (c), with dual vertices. Line weights indicate stress signs.

*Proof.* The first assertion follows from Lemma 5 and the fact that the clockwise and counterclockwise angles between two edges add up to  $2\pi$ .

For the second assertion, the equation that we now have is  $2n\pi - (k - 2)\pi - s\pi = 2\pi$ , where  $k$  and  $s$  again are the number of corners and vertex-proper sign changes respectively. This equation reduces to  $s + k = 2n$ , which implies  $s = k = n$ . So  $F$  is a convex polygon with all signs equal, as stated.

In particular, an angle of  $\pi$  with no sign change will make the two reciprocal edges overlap at the reciprocal vertex. Any angle of  $\pi$  with a non-crossing reciprocal must have a sign change. This means such angles cannot occur in the reciprocal with the same orientation. The polygon is strictly convex.  $\square$

## 2.2. Combinatorial Conditions for a Non-Crossing Reciprocal

Observe that in the description above,  $F$  was implicitly assumed to be an interior face. As mentioned before, orientations of the outer face have to be considered reversed, which means that the conditions of Lemmas 5 and 6 have to be interchanged when looking at the outer face. Hence:

**Theorem 2.** *It is impossible for a non-crossing framework to have a non-crossing reciprocal with the same orientation.*

*Proof.* According to Lemma 6, all interior faces should be convex and all edges should have the same sign. However, according to Lemma 5, the outer face must have some sign changes: at convex hull vertices we have vertex-proper sign changes if consecutive edges have the same sign. There are at least three convex hull vertices, but only one vertex proper sign change is allowed.  $\square$

Hence, every pair of non-crossing reciprocals will have opposite orientations. Then Lemmas 5 and 6 imply:

**Theorem 3** (Face Conditions for a Non-Crossing Reciprocal). *Let  $(G, \rho)$  be a non-crossing framework with given self-stress  $\omega$ . The following face conditions on the signs of  $\omega$  are necessary in order for the reciprocal framework  $(G^*, \rho^*)$  to be also non-crossing:*

- (1) *The (complement of) the exterior face is strictly convex with no sign changes.*
- (2) *The internal faces of  $(G, \rho)$  are either*
  - (a) *pseudo-triangles with two sign changes, both occurring at corners,*
  - (b) *pseudo-triangles with four sign changes, three occurring at corners, or*
  - (c) *pseudo-quadrangles with four sign changes, all occurring at corners.*

Theorem 3 says in particular that if two reciprocal frameworks are both non-crossing, then they are both pseudo-quadrangulations.

Of course, the conditions on faces of  $(G, \rho)$  translate into conditions on the vertices of  $(G^*, \rho^*)$ . For both frameworks to be non-crossing, both sets of conditions must

be satisfied in each framework. In particular, the following vertex conditions must be satisfied in  $(G, \rho)$ :

**Theorem 4** (Vertex Conditions for a Non-Crossing Reciprocal). *Let  $(G, \rho)$  be a non-crossing framework with given self-stress  $\omega$ . Then, in order for the reciprocal framework  $(G^*, \rho^*)$  to be also non-crossing, the following vertex conditions need to be satisfied by the signs on its vertex cycles:*

- (1) *There is a non-pointed vertex with no sign changes.*
- (2) *All other vertices are of one of the following three qualities:*
  - (a) *Pointed vertices with two sign changes, none of them at the big angle.*
  - (b) *Pointed vertices with four sign changes, one of them at the big angle.*
  - (c) *Non-pointed vertices, including any vertices with a flat angle, with four sign changes.*

*Moreover, vertices of  $(G, \rho)$  in each of the cases (1), (2a), (2b) and (2c) correspond respectively to faces of  $(G^*, \rho^*)$  in the corresponding parts of Theorem 3, and vice versa.*

*Proof.* Each of the cases of Theorem 3, applied to a face in  $(G^*, \rho^*)$ , gives the condition stated here for the reciprocal vertex of  $(G, \rho)$ . See Figs. 11 and 12.  $\square$

We show below that the vertex conditions of Theorem 4 actually imply the face conditions of Theorem 3.

Both the face and the vertex conditions admit a simple rephrasing in terms of vertex-proper and face-proper angles. Namely:

- (1) The face conditions say that there is exactly one vertex-proper angle in every pseudo-triangle, and no vertex-proper angle in the pseudo-quadrangles and the outer face.
- (2) The vertex conditions say that there are exactly three face-proper angles at every pointed vertex and four at every non-pointed vertex other than the one reciprocal to the outer face, which has no face-proper angle.

Observe that a pseudo- $k$ -gon with  $k$  even (resp.,  $k$  odd) must have an even (resp., odd) number of vertex-proper angles, simply because it has an even number of sign changes. Hence, the face conditions say that this number is as small as possible: zero for pseudo-quadrangles and the outer face, one for pseudo-triangles.

Similarly, the number of face-proper angles around a non-pointed (resp., pointed) vertex must be even (resp., odd). Again, the vertex conditions say that this number is as small as possible for the distinguished non-pointed vertex and for all pointed vertices (but not for other non-pointed vertices), as the following result shows:

**Lemma 7.** *A self-stress produces at least three face-proper angles at every pointed vertex  $v$  (unless it is zero on all edges incident to  $v$ ).*

*Proof.* Observe that in order to meet the equilibrium condition around a vertex, no line can separate the positive edges of the self-stress incident to that vertex from the negative ones. In the case of a pointed vertex this rules out the possibility of having just one face-proper angle. Indeed, if the face-proper angle is at the big angle then all signs are equal, and a tangent line to the point does the job. If the face-proper angle is small, then a line through that angle does it. Since the number of face-proper angles at a pointed vertex is odd, it must be at least three.  $\square$

In Theorem 10 we prove an extra condition that the signs of a self-stress must satisfy in order to have a non-crossing reciprocal: the edges in the boundary cycle must have opposite signs to those around the distinguished non-pointed vertex (the one whose reciprocal is the outer face). The proof uses the relation between self-stresses and polyhedral liftings of frameworks.

### 2.3. Necessary and Sufficient Conditions

Unfortunately, the purely combinatorial conditions on the signs of the self-stress stated in Theorems 3 and 4 are not sufficient to guarantee that the reciprocal is non-crossing. Figure 13 depicts a framework and a self-stress satisfying these conditions, part (a), but its reciprocal, part (b), has crossings. We note that this example is a geometric circuit; in particular, it has a unique self-stress (up to a constant). Part (c) of the same figure shows a slightly different embedding of the same graph, for which the reciprocal, part (d), turns out to be non-crossing. We conclude that there can be no purely combinatorial characterization (that would depend only on the signs of the self-stress and on which angles are big/small) of frameworks with a non-crossing reciprocal.

It is easy to analyze what goes wrong in this example: the signs around the interior vertex of degree five in part (a) should produce a pseudo-quadrangle, but, instead, they produce a self-intersecting closed curve (which can be regarded as a “self-intersecting pseudo-quadrangle”). The following statement tells us that such self-intersecting pseudo-quadrangles are actually the only thing that can prevent a non-crossing framework with the appropriate signs in its self-stress from having a non-crossing reciprocal:

**Theorem 5.** *Let  $(G, \rho)$  be a non-crossing framework with a given self-stress  $\omega$ . The reciprocal is non-crossing if and only if the signs of the self-stress around every vertex*

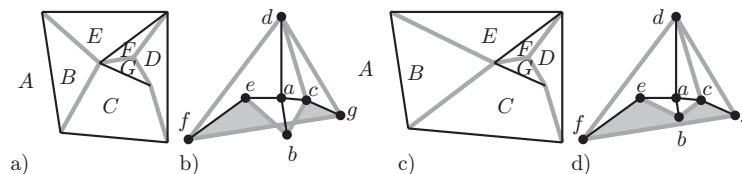


**Fig. 13.** Sign conditions are not enough to guarantee a non-crossing reciprocal. The geometric circuit in part (a) has the same signs (and big/small angles) as the one in part (c), but the former produces a crossing reciprocal (b) while the latter produces a non-crossing one (d).



satisfy the conditions of Theorem 4 and, in addition, the face cycles reciprocal to the non-pointed vertices with four sign changes are themselves non-crossing (and hence, pseudo-quadrangles).

*Proof.* That the reciprocal cycles of every vertex of  $(G, \rho)$  need to be non-crossing for the reciprocal to be non-crossing is obvious. The reason why we only impose the condition on vertices of type (2c) is that the reciprocal cycles of vertices of types (1), (2a) and (2b) are automatically non-crossing: there are no self-intersecting convex polygons or pseudo-triangles.

Let us see sufficiency. The conditions we now have on vertex cycles tell us that we have a collection of simple polygons (one of them exterior to its boundary cycle, containing all the “infinity” part of the plane) and that these polygons can locally be glued to one another: for every edge of every polygon there is a well-defined matching edge of another polygon. Moreover, the fact that the orientations are all consistent implies that the two matching polygons for a given edge lie on opposite sides of that edge.

If we glue all these polygons together (which can be done for any reciprocal, non-crossing or not) what we get is a map from the topological dual of the framework  $(G, \rho)$  (with a point removed, in the interior of the face reciprocal to the distinguished non-pointed vertex) to the Euclidean plane. The local argument shows that this map is a covering map, except perhaps at vertices where in principle the map could wind-up two or more complete turns. However, the covering map clearly covers infinity once, hence by continuity it covers everything once. This implies that the map is actually a homeomorphism. That is, that the reciprocal framework is non-crossing.  $\square$

One can interpret the meaning of the extra condition in Theorem 5 for the values of the self-stress more explicitly. Observe that a closed cycle is self-intersecting if and only if it can be decomposed into two cycles. Reformulated as an assertion about a vertex  $v$  of  $(G, \rho)$  this means that there are two edges  $e$  and  $e'$  around  $v$  such that the self-stress (restricted to the edges around  $v$  and the equilibrium condition at  $v$ ) can be “split” into two self-stresses, one supported on the edges on one side of  $e$  and  $e'$  and the other on the edges on the other side.  $e$  and  $e'$  may be used in both self-stresses, but if so, they must have the same sign they have in the original self-stress.

To see this equivalence, just remember how to construct the reciprocal cycle of a given self-stressed vertex: consider all edges incident to  $v$  oriented going out of  $v$  and then place them one after another (the end of one coinciding with the beginning of the next one), scaling each edge by the value of the self-stress on that edge; in particular, reversing the edge if the self-stress is negative.

It is interesting to observe that Theorem 5 does not explicitly require that the framework be a pseudo-quadrangulation, that is a consequence of the hypotheses. Corollary 1 below shows that the vertex conditions alone suffice.

**Lemma 8.** *Let  $(G, \rho)$  be a pseudo-quadrangulation with  $e$  edges,  $t$  pseudo-triangles,  $q$  pseudo-quadrangles,  $y$  pointed vertices and  $x$  non-pointed vertices. In a self-stress of  $(G, \rho)$ , the following five properties are equivalent:*

- (1) *The face conditions of Theorem 3.*

- (2) *There are exactly  $t$  vertex-proper angles.*
- (3) *There are at most  $t$  vertex-proper angles.*
- (4) *There are exactly  $3y + 4x - 4$  face-proper angles.*
- (5) *There are at least  $3y + 4x - 4$  face-proper angles.*

*Proof.* By Lemma 1,  $2e = t + 3y + 4x - 4$ , where  $2e$  is the total number of angles, so conditions (2) and (3) are equivalent to (4) and (5), respectively.

For (1)  $\Rightarrow$  (2) observe that the face conditions can be rephrased as “there is exactly one vertex-proper angle in each pseudo-triangle, and no vertex-proper angle in a pseudo-quadrangle or in the outer face”. For the converse, (2)  $\Rightarrow$  (1), recall that we always have at least  $t$  vertex-proper angles, one at each pseudo-triangle. The face conditions are just saying that there are no more. The same observation gives (2)  $\Leftrightarrow$  (3).  $\square$

**Corollary 1.** *Let  $(G, \rho)$  be a non-crossing framework, and let  $\omega$  be any sign assignment satisfying the vertex conditions of Theorem 4. Then the face conditions of Theorem 3 also hold. In particular,  $(G, \rho)$  is a pseudo-quadrangulation.*

*Proof.* Let  $t$  denote the number of pseudo-triangles in  $(G, \rho)$ , and let  $q$  be the number of other bounded faces (it will soon follow that they have to be pseudo-quadrangles, but we do not explicitly require this). The same counting argument of Lemma 1 yields the inequality  $2e \geq 3t + 4q + y$ , with equality if and only if we have a pseudo-quadrangulation. Together with Euler’s formula we obtain  $2e \leq t + 3y + 4x - 4$ , with equality for pseudo-quadrangulations.

Now, the vertex conditions imply  $3y + 4x - 4$  face-proper angles and we have at least  $t$  vertex-proper angles (one in each pseudo-triangle). Hence,  $2e \geq t + 3y + 4x - 4$ , which means that all the inequalities mentioned so far are tight and we have a pseudo-quadrangulation satisfying the face conditions.  $\square$

#### 2.4. Three Special Cases

Something more precise can be said if  $(G, \rho)$  is either a geometric circuit, or a pseudo-triangulation, or if it has a unique non-pointed vertex. Observe that the first case is self-reciprocal and the other two are reciprocal to each other.

We start with the case of a framework with a single non-pointed vertex. Recall that the dimension of the space of self-stresses in a non-crossing framework is bounded above by the number of non-pointed vertices. At least one non-pointed vertex is needed to sustain a self-stress. The presence of exactly one non-pointed vertex implies the existence of a unique self-stress. We call frameworks with only one non-pointed vertex *almost pointed*. The crucial feature about this case is that the extra condition introduced in Theorem 5 is superfluous. The reciprocal is always non-crossing.

**Corollary 2.** *Let  $(G, \rho)$  be a non-crossing framework with a self-stress and a single non-pointed vertex. Then the reciprocal framework is non-crossing. In particular,  $(G, \rho)$  is a pseudo-quadrangulation. Moreover, if the self-stress is everywhere non-zero, then*

*the reciprocal is a pseudo-triangulation with  $q + 1$  non-pointed vertices, where  $q$  is the number of pseudo-quadrangles in  $(G, \rho)$ .*

Assuming that the self-stress is everywhere non-zero is actually no loss of generality: the reciprocal of a singular self-stress is just the reciprocal of the subgraph of non-zero edges. However, we need it in the second part of the statement in order to get the correct count of pseudo-quadrangles.

*Proof.* Let  $t$  be the number of pseudo-quadrangles and let  $q$  be the number of other faces. As in the previous corollary,  $2e \leq t + 3y + 4x - 4 = t + 3y$ , with equality if and only if we have a pseudo-quadrangulation. However, we do have equality, since we have at least  $t$  vertex-proper angles (one per pseudo-triangle) and at least  $3y$  face-proper angles, by Lemma 7. The equality implies that the vertex conditions are satisfied, hence the reciprocal is non-crossing.

The fact that the reciprocal is a pseudo-triangulation with  $q + 1$  non-pointed vertices is trivial. The reciprocals of pointed vertices are pseudo-triangles, and the reciprocals of pseudo-quadrangles and of the outer face are non-pointed vertices.  $\square$

Now we look at pseudo-triangulations. The first observation is that not all pseudo-triangulations have self-stresses that produce non-crossing reciprocals. For example, the ones in Fig. 14 cannot have self-stresses satisfying the vertex conditions, because those conditions forbid more than one non-pointed vertex of degree three. It is also interesting to observe that these pseudo-triangulations possess self-stresses satisfying the face conditions. For example, put negative stress to all edges incident to non-pointed vertices of degree three, and positive stress on the others.

**Corollary 3.** *Let  $(G, \rho)$  be a pseudo-triangulation with  $x$  non-pointed vertices and a self-stress yielding a non-crossing reciprocal. Then this reciprocal has one non-pointed vertex,  $x - 1$  pseudo-quadrangles and  $n - x$  pseudo-triangles.*

*Proof.* Straightforward, from Theorem 4.  $\square$

Finally, we look at geometric circuits. Again, not all have non-crossing reciprocals, as Fig. 1 shows.

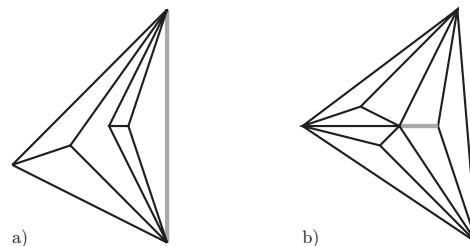


**Fig. 14.** These pseudo-triangulations have a self-stress fulfilling all face conditions but do not have a good self-stress.

**Corollary 4.** *Let  $(G, \rho)$  be a geometric circuit. That is,  $G$  is a Laman circuit and  $(G, \rho)$  is a non-crossing framework with a non-singular self-stress. If a reciprocal  $G^*$  is non-crossing, then the numbers of pseudo-triangles, pseudo-quadrangles, pointed vertices and non-pointed vertices are the same in  $G$  and  $G^*$ .*

*Proof.* We use the formula  $2e = t + 3y + 4x - 4$  of Lemma 1. Since a Laman circuit has  $e = 2n - 2 = 2x + 2y - 2$  edges, we get  $y = t$ . However,  $t$  is also the number of pointed vertices in the reciprocal and  $y$  is the number of pseudo-triangles in it. Now, by Euler's formula,  $q + t + n - 1 = e = 2n - 2$ , hence  $q + t = n - 1$  and  $q = n - t - 1 = n - y - 1 = x - 1$ . That is to say,  $q = x - 1$  and  $x = q + 1$ . Again,  $x - 1$  is the number of pseudo-quadrangles in the reciprocal, and  $q + 1$  is the number of non-pointed vertices.  $\square$

### 3. Laman Circuit Pseudo-Triangulations Have Non-Crossing Reciprocals

#### 3.1. The Non-Singular Case (Geometric Circuit Pseudo-Triangulations)

We start with a geometric circuit pseudo-triangulation. That is to say, a Laman circuit embedded as a pseudo-triangulation with one non-pointed vertex whose self-stress is non-zero on every edge. This simultaneously satisfies the hypotheses of Corollaries 2–4. Hence:

**Theorem 6.** *The reciprocal of a Laman circuit pseudo-triangulation with non-singular self-stress is non-crossing and again a Laman circuit pseudo-triangulation (Fig. 15).*

Together with Theorem 1, Theorem 6 implies:

**Theorem 7.** *Let  $G$  be a Laman circuit. The following are equivalent:*

- (1)  $G$  is planar.
- (2)  $G$  has a planar embedding with a non-crossing reciprocal.
- (3)  $G$  can be embedded as a pseudo-triangulation with one non-pointed vertex (whose reciprocal is, in turn, a pseudo-triangulation with one non-pointed vertex if the embedding is generic).

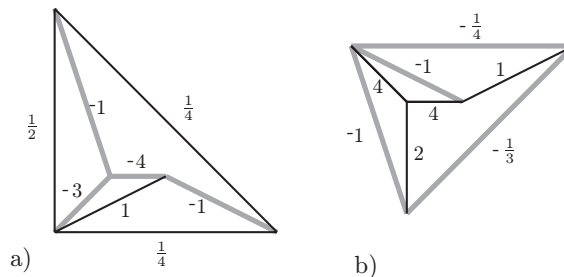


**Fig. 15.** A reciprocal pair of Laman circuit pseudo-triangulations.

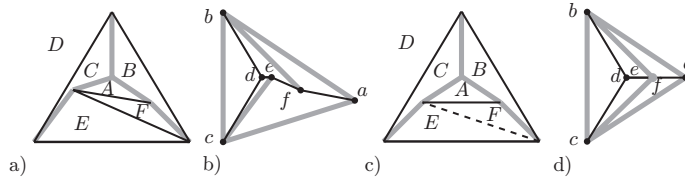


**Fig. 16.** A singular self-stress on a Laman circuit pseudo-triangulation can drop an edge from the original graph—and fuse two vertices in the reciprocal.

### 3.2. Singular Circuit Pseudo-Triangulations

For a given planar Laman circuit  $G$ , the embeddings  $\rho$  creating a pseudo-triangulation  $(G, \rho)$  form an open subset of  $\mathbb{R}^{2|V|}$ . The non-singular pseudo-triangulations of Section 3.1, which are geometric circuits, form an open dense subset of this subset. The remaining singular pseudo-triangulations are “seams” between some components of this open dense set.

Consider any singular pseudo-triangulation on a Laman circuit. The self-stress is supported on a subgraph  $G_s$ , see Fig. 16(a). Since this framework is still infinitesimally rigid with  $|E| = 2|V| - 2$ , it has a one-dimensional space of self-stresses. This framework  $(G_s, \rho_s)$  with its self-stress can be approached as a limit of geometric circuits  $(G, \rho_n)$  on the whole graph, each with a planar reciprocal by Section 3.1. One can anticipate that the limit of these reciprocals will also be non-crossing, and this is what we prove below.

For example, when an edge drops out of the self-stress, the two faces separated by the lost edge become one face in the subgraph  $G_s$ , see Figs. 16(a), (c). For each lost edge of the original, the corresponding edge of the reciprocal, whose length records the coefficient in the self-stress, will shrink to zero, and the two reciprocal vertices are fused into one vertex corresponding to the unified face of the original. See Figs. 16(b), (d).

We now prove that even in these singular situations the reciprocal is non-crossing and a pseudo-triangulation.

**Theorem 8.** *Let  $(G, \rho)$  be Laman circuit embedded as a (possibly singular) pseudo-triangulation. Then it has a unique self-stress, supported on a subgraph  $G_s \subseteq G$ .  $G_s$  is a pseudo-quadrangulation with a unique non-pointed vertex and with  $q = 2n - 2 - e$  pseudo-quadrangles, if  $G_s$  has  $e$  edges and spans  $n$  vertices. Its reciprocal is non-crossing, and it is a pseudo-triangulation with  $n - 1$  pseudo-triangles and  $q + 1$  non-pointed vertices.*

*Proof.* By Lemma 1  $(G, \rho)$  has a unique non-pointed vertex. Clearly, vertices of  $G_s$  that were pointed in  $(G, \rho)$  are pointed also in  $(G_s, \rho)$ . In particular,  $G_s$  has at most one non-pointed vertex. By Corollary 2, the reciprocal is non-crossing. The other statements are easy to verify. □

### 3.3. Good Self-Stresses

We have seen that all reciprocals corresponding to a (possibly singular) self-stress on a Laman circuit are non-crossing pseudo-triangulations. We say that a self-stress on a

non-crossing framework  $(G, \rho)$  is a *good self-stress* if it is non-zero on all edges and the reciprocal for this self-stress is non-crossing. The existence of a good self-stress is precisely equivalent to the existence of a non-crossing reciprocal with all edges of non-zero length. Does the construction in Theorem 8 create all examples of a good stress on a pseudo-triangulation? The answer is yes.

**Theorem 9.** *If a pseudo-triangulation  $(G^*, \rho^*)$  has a good self-stress, then  $(G^*, \rho^*)$  is the reciprocal of a (possibly singular) Laman circuit pseudo-triangulation  $(G, \rho)$ .*

*Proof.* Let  $(G_s, \rho)$  be the reciprocal of  $(G^*, \rho^*)$ , which is non-crossing by assumption. By Corollary 3,  $(G_s, \rho_s)$  is an almost pointed framework, with pseudo-triangles and pseudo-quadrangles. If  $(G_s, \rho_s)$  is already a pseudo-triangulation, then both graphs are Laman circuits, and we are finished. Otherwise there are some pseudo-quadrangles.

As is well-known, a “diagonal” edge can be added through the interior of each pseudo-quadrangle to subdivide it into two pseudo-triangles, such that no new non-pointed vertex is created [20, Theorem 6]. This process creates a pseudo-triangulation  $(G, \rho_s)$ , with one non-pointed vertex and the same vertex set as  $(G_s, \rho_s)$ .

Such an almost-pointed pseudo-triangulation  $(G, \rho_s)$  has a unique self-stress, in this case the self-stress supported on  $G_s$ . That is to say,  $(G^*, \rho^*)$  is not only the reciprocal of  $(G_s, \rho_s)$ , but also of the almost-pointed pseudo-triangulation  $(G, \rho_s)$  with singular self-stress.  $\square$

A singular self-stress can drop not only edges of the original pseudo-triangulation but also vertices (Fig. 17). However, it is a consequence of this proof that we can choose some alternate pseudo-triangulation in which the singular self-stress spans all vertices. In that case, some simple counting arguments give more information on the connections between  $(G, \rho_s)$  and the support  $(G_s, \rho_s)$  of the singular stress.

**Corollary 5.** *Let  $(G, \rho)$  be a Laman circuit pseudo-triangulation, and let  $G_s$  be a spanning subgraph of  $G$  supporting a self-stress. Let  $k$  be the number of edges not used in  $G_s$ , so that  $|E_s| = 2|V_s| - 2 - k$ ,  $k > 0$ . Then:*

- (1)  $(G_s, \rho)$  is a pseudo-quadrangulation with  $n - 1 - 2k$  pseudo-triangles and  $k$  pseudo-quadrangles, each formed as the union of two pseudo-triangles of  $(G, \rho)$ .

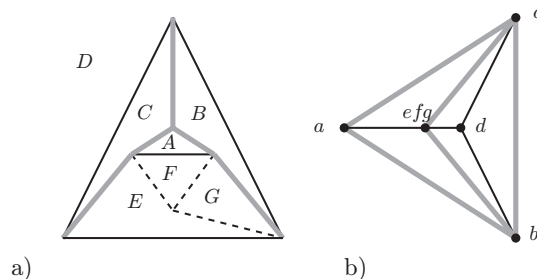


**Fig. 17.** A singular stress on a Laman circuit can drop both vertices and edges.

- (2) *The non-pointed vertex of  $(G, \rho)$  is still non-pointed in  $(G_s, \rho)$ , and  $(G_s, \rho)$  contains the boundary cycle of  $(G, \rho)$ .*
- (3) *The reciprocal is a pseudo-triangulation with  $k + 1$  non-pointed vertices.*

*Proof.* The  $n - 1$  pointed vertices of  $G$  are still pointed in  $G_s$ . Hence, they still have at least  $3n - 3$  face-proper angles. Since every edge is incident to two faces, the removal of  $k$  edges destroys at most  $2k$  pseudo-triangles, hence we still have at least  $n - 1 - 2k$  pseudo-triangles, each with at least one vertex-proper angle. These  $(3n - 3) + (n - 1 - 2k) = 2(2n - 2 - k)$  angles equal twice the number of edges in  $G_s$ . In particular, the number of pseudo-triangles of  $G$  that survived in  $G_s$  is exactly  $n - 1 - 2k$ , and there is no other pseudo-triangle in  $G_s$ . Therefore, each of the  $k$  removed edges merged two pseudo-triangles into a pseudo-quadrangle, and the  $2k$  merged pseudo-triangles are all different. This proves parts (1) and (2) (the latter because if the removal of an edge makes the non-pointed vertex pointed, then this removal merges two pseudo-triangles into a pseudo-triangle, not a pseudo-quadrangle).  $\square$

#### 4. The Spatial Liftings of Non-Crossing Reciprocal Pairs

A self-stress on a framework  $(G, \rho)$  defines a lifting of the framework into 3-space with the property that face cycles are coplanar. Here we look at the lifting produced by a *good self-stress*; that is, a self-stress on a non-crossing framework that produces a non-crossing reciprocal. For any non-crossing framework, the lifting is a polyhedral surface with exactly one point above each point of the plane (we emphasize that the outer face is considered exterior to its boundary cycle; the standard Maxwell lifting would consider it interior to the cycle, hence providing a closed, perhaps self-intersecting surface, with two points above each point inside the convex hull of the framework). The lifting is unique up to a choice of a first plane and of which sign corresponds to a valley or a ridge [6], [7], [26]. Our standard choice for the starting plane places the exterior face horizontally at height zero, and our standard choice for signs sets the edges in the boundary cycle as valleys. The latter makes sense since in a good self-stress all boundary edges have the same sign. We call this the *standard lift*  $(G, \mu)$  of the good self-stress  $(G, \rho)$ .

Figures 4, 20 and 21 show standard liftings of several good self-stresses. In all of them one observes a similar “shape”: the entire surface curls upwards from the base to a single maximum point, which is the lifting of the distinguished non-pointed vertex. In particular, there are no local maxima other than this peak, or local minima except the exterior face in such a surface. The main theorem in this section shows that these claims hold for all lifts of non-crossing frameworks with non-crossing reciprocals.

For this spatial analysis it is easier to reason with the *Maxwell reciprocal*, in which each reciprocal edge is perpendicular, instead of parallel, to the original edge. This Maxwell reciprocal is obtained by rotating the Cremona reciprocal by  $90^\circ$ . The reason for the rotation is that given a spatial lifting a Maxwell reciprocal is created by choosing one central point in 3-space—for example  $(0, 0, 1)$ —and drawing normals to each of the faces through this point. The intersection of the normal to face  $F$  with the plane  $z = 0$  is then the reciprocal vertex for this face [6], [7]. If we want to ensure, for visual clarity, that the reciprocal and the original framework do not overlap, we simply translate this

construction off to the right by picking the central point to be  $(t, 0, 1)$ . This is what we have done in our figures.

**Theorem 10.**

- (i) *Given a non-crossing framework  $(G, \rho)$  with a self-stress such that the corresponding reciprocal  $(G^*, \rho^*)$  is non-crossing, the standard lifting  $(G, \mu)$  has a unique local (and global) maximum point, whose reciprocal is the boundary of  $(G^*, \rho^*)$ , and has all signs in the self-stress opposite to those on the original boundary.*
- (ii) *The maximum is the unique point where the lifted surface is “pointed”, meaning that a hyperplane exists passing through it and leaving a neighborhood of it in one if its two open half-spaces.*
- (iii) *The boundary face is the unique local minimum of  $(G, \mu)$ .*

*Proof.* In the standard lifting, the boundary is a horizontal plane and every edge is attached to an upward sloping face. No local maximum can be on the boundary.

Take any isolated local maximum. Cut the lifted surface, just below this point, with a horizontal plane. This cuts off a pyramid whose vertical projection is a non-crossing wheel framework. Because of the spatial realization, this projection is a reduced non-crossing framework  $(W, \rho_w)$  (Fig. 18) which has a corresponding reduced reciprocal, also, graphically, a wheel. At this hub vertex, the pyramid and the original surface have the same face planes and edges. Therefore, this hub has the same reciprocal polygon in the wheel reciprocal and in the original reciprocal  $(G^*, \rho^*)$ , and the same stresses along these edges in the two projections. Moreover, the signs of the spokes in this stress indicated the concavity or convexity of the edge in the lifting  $\mu$  and the concavity or convexity in the rim polygon at this spoke of the wheel. We can now sweep around the maximal hub: we start with the plane of a face, then we rotate the plane about an adjacent spoke until we reach the next face, etc. The normals to these tangent planes track the reciprocal polygon, with a reciprocal vertex for the normal to each of the faces.

If the base of the pyramid is not a convex polygon, then there is some segment of the convex hull between two vertices of the base polygon which does not lie in the polygon, placing all other vertices into one half-plane (Fig. 18(b)).

Consider the plane  $Q$  formed by this segment and the hub in space. This plane will place all of the pyramid in one half-space, touching it in at least two spokes. We claim

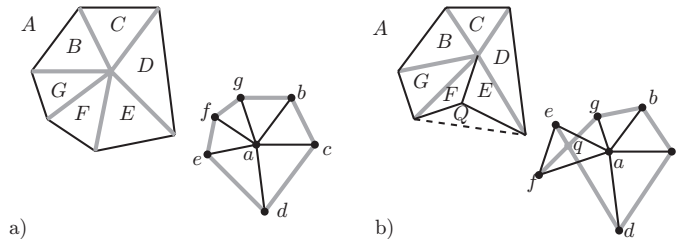


**Fig. 18.** Possible pyramids which might be created by a cut near a maximum in the lifting of a non-crossing framework (shown in vertical projection), with their reciprocals.



that the normal  $q$  to this plane is a crossing point of the reciprocal polygon. As we sweep around a spoke that lies in  $Q$ , we will encounter  $Q$  as one of the tangent planes, and hence  $q$  will appear on the edge reciprocal to the spoke. Since this happens for at least two spokes, the reciprocal polygon is self-intersecting at  $q$ .

Since we know that the reciprocal polygon is non-crossing (and non-touching) we conclude that the original pyramid base must be a convex polygon. A direct analysis of the wheel now guarantees that all the signs of the spokes of the wheel are the same—and are opposite to the rim of the wheel, representing ridges. Since the stress, and the signs, at the hub are the same in the larger framework, we conclude that any maximal vertex has all signs the same, and these signs are opposite to the boundary of the framework.

By Theorem 4, we know that there is only one vertex with no sign changes in each side of a reciprocal pair of non-crossing frameworks, and that this vertex is the reciprocal of the boundary of the other framework in the pair. We conclude that there is a unique local maximum—the global maximum. This global maximum corresponds to the convex boundary polygon in the reciprocal. Thus we have proved part (i) of the theorem for a local maximum consisting of an isolated vertex.

If we can cut off a vertex  $v$  of the lifting with a plane  $P$  which is not necessarily horizontal, but cuts all edges between  $v$  and its neighbors, the above argument applies without change. This section will still produce a spatial wheel which will project into a plane wheel with the hub inside the rim. Any such vertex would have to be the reciprocal vertex of the boundary, and since this vertex is unique, we have proved statement (ii) of the theorem.

Let us consider the case in which a local maximum is not just a vertex but a larger connected set  $M$  consisting of horizontal lines and horizontal faces. We can apply the argument of the previous paragraph to any vertex of the convex hull of  $M$ .

Given any local minimum that is not on the boundary, the same argument about the pyramid cut, and the sense of the reciprocal polygon applies. This gives a contradiction, so the only local minimum is along the boundary face, proving part (iii).  $\square$

Statement (ii) can be interpreted as saying that the maximum is the only (locally) strictly convex vertex of the surface. However, it is possible for a vertex  $v$  to have all adjacent vertices in a *closed* half-space through  $v$ . This can only happen for a pointed vertex and the half-space bounded by the plane of the face into which it points. In particular, all boundary vertices have this property.

We can derive the following consequences of the previous theorem:

**Corollary 6.** *In a good self-stress, the edges incident to the distinguished non-pointed vertex are signed opposite to the edges of the boundary cycle.*

*Proof.* Since the distinguished vertex is the maximum of the standard lifting, some (hence all) of its incident edges are ridges, while the boundary edges are valleys in the standard lifting.  $\square$

**Corollary 7.** *In the lifting of a good self-stress there are no (horizontal) saddle points. All level curves are simple closed curves, and as we increase the height the level*

curve moves monotonically from the boundary cycle to the distinguished non-pointed vertex.

Observe, however, that the intermediate level curves need not be convex, even though the boundary cycle and the level curves sufficiently close to the tip are convex. For example, this happens in Fig. 20.

*Proof.* There cannot be any saddle points, because general Morse theory on a disk with a horizontal boundary shows that a saddle point would require an additional local maximum or a new local minimum. In the absence of saddle points, Morse theory also implies that all level curves are isotopic to one another, hence they are all simple closed curves because the boundary cycle is.  $\square$

**Theorem 11.** *For any vertex except the maximum, there is a plane through that vertex that cuts the neighborhood into four pieces, just like a tangent plane through a saddle point. No plane through a vertex cuts the neighborhood into more than four pieces, i.e. there are no multiple saddles.*

*More precisely, for every general direction in the interior of the reciprocal figure there is a unique vertex such that a plane with this normal through the vertex cuts the neighborhood into four pieces. For planes with this normal, all other vertex neighborhoods are cut into two pieces, with the exception of the peak, whose neighborhood lies entirely below the plane. For all directions in the outer face of the reciprocal, a plane with that normal will cut the neighborhood of every vertex, including the peak, into two pieces.*

*Proof.* The neighborhood of  $v$  consists of an alternating cyclic sequence of edges emanating from  $v$  and faces between those edges; in the face  $V^*$  reciprocal to  $v$ , these correspond to vertices and edges, respectively.

We want to count how many faces incident to  $v$  meet a given plane  $Q$  through  $v$ . In order to determine whether  $Q$  intersects a given face  $F$  between two neighboring edges  $e_1$  and  $e_2$  emanating from  $v$ , we look at the relation between the reciprocal normal vector  $q^*$  and the reciprocal vertex  $f^*$ , forming an angle of  $V^*$  with the incident edges  $e_1^*$  and  $e_2^*$ . It turns out that  $Q$  intersects  $F$  if and only if

- $e_1^*$  and  $e_2^*$  have different signs and the line through  $q^*$  and  $f^*$  cuts through the boundary of  $V^*$  at  $f^*$ , or
- $e_1^*$  and  $e_2^*$  have the same sign and the line through  $q^*$  and  $f^*$  is tangent to the boundary of  $V^*$  at  $f^*$ .

We know that the signs around  $V^*$  satisfy the face conditions. It follows that  $q^*$  has the above-mentioned relation to precisely four vertices of a face  $V^*$  if  $q^*$  lies in  $V^*$ , and to precisely two vertices of  $V^*$  if  $q^*$  lies outside  $V^*$ . This holds for the interior faces of the reciprocal (pseudo-triangles and pseudo-quadrangles), and it can be easily proved by checking a few elementary cases and then showing that the number of “related” vertices does not change as one moves  $q^*$ , except when crossing the boundary of  $V^*$ .

When  $v$  is the peak and  $V^*$  is the outer face,  $q^*$  is related to precisely two vertices of  $V^*$  if it lies in the outer face, and to no vertices otherwise.

The desired statements now follow easily. (The first part of the theorem, which is only a local statement about the neighborhood of  $v$ , can also be proved directly in the original framework along the lines of the proof of Theorem 10 by considering the geometry and the possible sign patterns of edges between two intersections with  $Q$ .)  $\square$

The behavior exhibited in the previous corollary is analogous to what happens in the upper half of the *pseudo-sphere*, a surface of constant negative curvature in 3-space which serves as a model for (a part of) the hyperbolic plane. The pseudo-sphere is the surface of revolution generated by a tractrix. The upper half is given in parametric form in polar coordinates  $r, \varphi, z$  by the equations  $z = u - \tanh u, r = \operatorname{sech} u$  for  $u \geq 0$ . When the pseudo-sphere is viewed as the graph of a function over the unit circle, then for every gradient direction there is a unique point with that gradient, and the mapping *point*  $\longleftrightarrow$  *gradient* is an orientation-reversing mapping between the pseudo-sphere and the plane. Also the properties in Theorem 10 confirm that the lifted surface of each framework in a non-crossing pair has the shape of a rough piecewise-linear pseudo-sphere, except that the pseudo-sphere has the vertical axis as an asymptote, whereas our lifted surface reaches a finite maximum. (In this sense the surface  $z = (r - 1)^2$  over the region  $r \leq 1$  might be a more appropriate smooth model for our lifted surface. It has a constant negative Laplacian  $\Delta z = -2$ .) In a visible sense, this lifted surface is as non-convex as possible.

Liftings of pseudo-triangulations have also emerged recently in the context of *locally convex* piecewise-linear functions over a polygonal domain subject to certain height restrictions [1]. There are some similarities, in particular regarding the twisted saddle property discussed in Theorem 11, but we have not explored whether there are any deeper connections to our present work.

## 5. Open Problems

Throughout this section we say that a non-crossing framework is *good* if it has some good self-stress, i.e. an everywhere non-zero stress that produces a non-crossing reciprocal. In particular, every almost pointed non-crossing framework is good. We do not require *all* its self-stresses to be good, simply because every framework with at least two (linearly independent) self-stresses has some bad self-stresses. Indeed, let  $\omega_1$  and  $\omega_2$  be two independent everywhere non-zero self-stresses on a framework, and suppose they are both good. Consider the associated standard liftings,  $\mu_1$  and  $\mu_2$ . For  $c > 0$  sufficiently big (resp., sufficiently small) the lifting  $c\mu_1$  lies completely above (resp., completely below)  $\mu_2$ . Since  $c\mu_1$  is never equal to  $\mu_2$ , there must be an intermediate value  $c_0$  for which  $c_0\mu_1$  has some parts above and some parts below  $\mu_2$ . In particular,  $c_0\omega_1 - \omega_2$  cannot be a good self-stress, because its associated lifting has parts above and below the plane of the outer face, which contradicts Theorem 10.

### 5.1. Good and Bad Pseudo-Triangulations

In Section 2 we saw examples of pseudo-triangulations which cannot support a good self-stress. In Fig. 19(b) we see a different framework on the same graph as in Fig. 14,

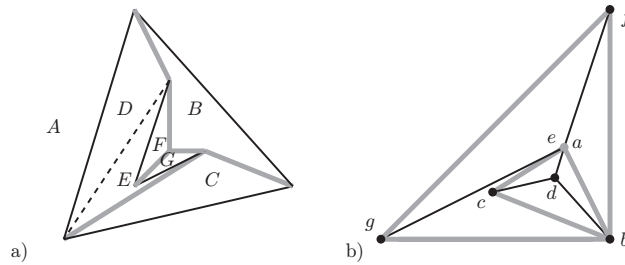


**Fig. 19.** A pseudo-triangulation with two non-pointed vertices (b) with its reciprocal (a), a singular pseudo-triangulation.

with the same face structure, which does have a good self-stress, as demonstrated by the non-crossing reciprocal. The difference between these examples lies in the choice of exterior face and of the associated big and small angles. In [17] a combinatorial analog of pseudo-triangulation is discussed in which the planar graph has a formal labeling of “big” and “small” assigned to the angles, which may or may not correspond to the big and small angles of any planar realization, with pseudo-triangle and pointedness described combinatorially.

For a given graph, having a good self-stress is an open property, so if there are any good realizations there are nearby generic realizations.

**Open Problem 1.** What conditions on a combinatorial pseudo-triangulation ensure existence of a good generic realization? If there is a good generic realization of a combinatorial pseudo-triangulation, are all generic realizations of this combinatorial pseudo-triangulation good? If the answer is yes, then a purely combinatorial characterization of combinatorial pseudo-triangulations that admit good embeddings should exist. Find it.

Observe that the second question has a negative answer if posed for pseudo-quadrangulations. Figures 20 and 22 show two different generic embeddings of a Laman circuit as pseudo-quadrangulations with the same big and small angles. The unique self-stress is good in the first embedding and bad in the second.

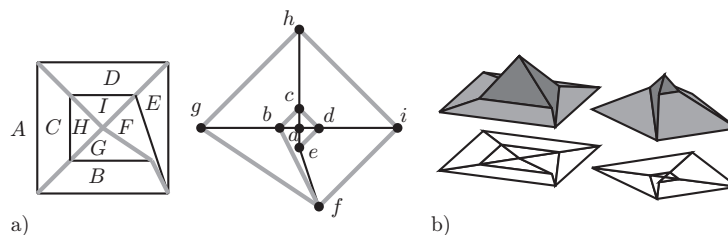


**Fig. 20.** A reciprocal pair of pseudo-quadrangulations on a Laman circuit.

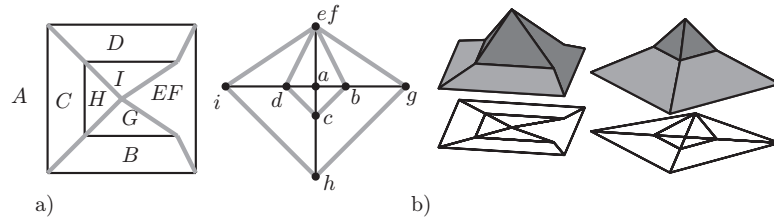


**Fig. 21.** A nearby singular framework with its compressed reciprocal and lift.

5.2. *Good Pseudo-Quadrangulations*

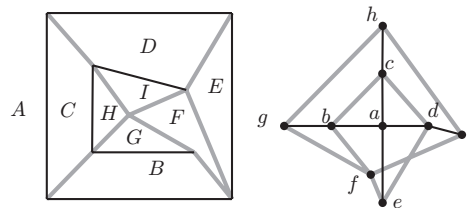
Our characterization in Section 2 applies to all non-crossing reciprocal pairs based on a graph  $G$  and its dual  $G^*$  on the induced face structure of the embedding. In general, these reciprocal pairs are composed of pseudo-triangles and pseudo-quadrangles, with at least one non-pointed vertex.

Figure 20(a) contains such a pair of non-crossing reciprocals on a Laman circuit, with the sign pattern of the corresponding self-stress, as predicted by Theorem 4, and Fig. 20(b) shows the lifts guaranteed by Maxwell’s theorem. Figure 21(a) contains a singular framework and its reciprocal (with two vertices fused) found as a limit from the previous example, with the sign pattern of the corresponding self-stress, as predicted by Theorem 3, and Fig. 21(b) shows the lifts. We note that a small additional change in location, away from the original pair across this singularity, can make this pseudo-quadrangulation bad, as the sign pattern is altered on the singular edge, see Fig. 22.

This illustrates that, once we leave the realm of pseudo-triangulations, the big and small angles are not sufficient to determine whether even a generic framework on a Laman circuit has a good self-stress.

**Open Problem 2.** Characterize directly by their geometric properties as embeddings, all non-crossing frameworks on a Laman circuit  $G$  with a non-crossing reciprocal.

Like all characteristics of a self-stress, the existence of a good self-stress on a framework is invariant under any *external projective transformation of the plane*, that is, a projective transformation in which the line being sent to infinity does not intersect any of



**Fig. 22.** The same graph and combinatorial pseudo-quadrangulation can be bad, because of an altered sign pattern.

the vertices or edges of the original framework. This invariance is a direct consequence of the map on the stress-coefficients induced by such a projective transformation, which does not change any signs and preserves all equilibria [21]. These two properties of the map guarantee that all the necessary and sufficient conditions of Section 2 are preserved.

However, whatever projective property is required for a good self-stress, it is more refined than the simple choice of large and small angles, or even the oriented matroid of the vertices themselves. We do not have a firm conjecture for the geometry in the framework which determines that there is a good self-stress. Such a good self-stress will be singular on any refinement of the framework to a pseudo-triangulation. The pure condition polynomials mentioned in the Introduction, which are zero for edges dropped in a singular self-stress, are projective invariants [25]. Recall Fig. 8, where the condition was the concurrence of three lines. It is possible that all the necessary information lies in the geometry of singular self-stresses on a pseudo-triangulation refining the pseudo-quadrangulation.

### 5.3. Refinement

It is natural to start with a non-crossing Laman circuit pseudo-triangulation and generate denser examples by adding edges. However, the refinement process does not preserve “goodness” in general, even when it adds no vertices.

In Fig. 23 we show an example of this. The framework on the left, without the edge  $cd$ , is an almost-pointed pseudo-triangulation, whose unique self-stress is by our results good (its reciprocal is on the right). We claim that if we add the edge  $cd$  then there is no good everywhere-non-zero self-stress on the framework. To see this, let  $\omega_1$  be the self-stress of the pseudo-triangulation and let  $\omega_2$  be the self-stress with support on the subgraph induced by the vertices  $a, b, c, d, e$  and  $g$  (including the edge  $cd$ ). Since this subgraph can be lifted to a roof-like surface,  $\omega_2$  has one sign, say negative, on the boundary and the opposite sign in the interior. Without loss of generality we assume that  $\omega_1$  was also negative on the boundary. It turns out that  $\omega_1$  and  $\omega_2$  generate the space of self-stresses

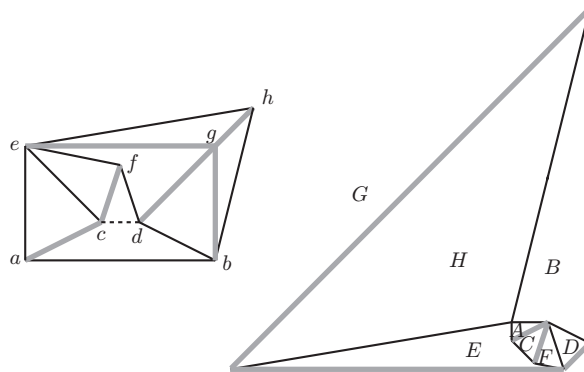


**Fig. 23.** A pseudo-quadrangulation with a good self-stress for which the added edge (dashed) makes a good self-stress on all edges impossible.

of the whole graph, but no linear combination  $\alpha\omega_1 + \beta\omega_2$  will give alternating signs to the edges of the quadrilateral  $abcd$ : if  $\alpha/\beta > 0$  then  $bd$  and  $cd$  get the same sign; if  $\alpha/\beta < 0$  then  $ac$  and  $cd$  do.

However, if a good pseudo-triangulation  $(G, \rho)$  is refined to another pseudo-triangulation  $(G', \rho)$  without adding vertices, we conjecture that  $(G', \rho)$  is good too. Our reason for this conjecture is that it is easy to prove that, at least, there is a self-stress in  $(G', \rho)$  satisfying the vertex conditions of Theorem 4. The idea of the proof is that one can go from  $(G, \rho)$  to  $(G', \rho)$  via a sequence of “elementary refinements” of one of the following types: addition of a single edge to divide a pseudo-triangle into two, or addition of three edges forming a triangle that separates the three corners of a pseudo-triangle, dividing it in four pseudo-triangles. (See Lemma 3 of [20] for a formal argument that these refinements are sufficient.) In both cases, a simple case study together with elementary properties of self-stresses gives the required sign pattern.

This conjecture reduces to proving that the extra condition ruling out bad quadrangles can be obtained too.

**Open Problem 3.** Is it true that every pseudo-triangulation refinement (with no extra vertices) of a good pseudo-triangulation is good?

Also, if one allows something more than simply adding edges:

**Open Problem 4.** To what extent can non-crossing reciprocal pairs be generated from Laman circuit pseudo-triangulations via refinement?

Solving either of these two problems could be a step toward solving Problem 1.

#### 5.4. *Lifting Questions*

Liftings of pseudo-triangulations have also emerged recently in the context of “locally convex” functions over a polygonal domain subject to certain height restrictions [1]. We have seen here that, given a pair of frameworks whose reciprocals are both non-crossing, the lifted surface of each framework shares some characteristic properties of a pseudo-sphere. It would be of interest to see if this resemblance increases with the density of the framework.

**Open Problem 5.** Let  $\{(G_i, \rho_i)\}$  be a sequence of Laman circuit pseudo-triangulations such that each  $(G_{i+1}, \rho_{i+1})$  is obtained from  $(G_i, \rho_i)$  by a making a Henneberg II move in a randomly selected face. With an appropriate normalization of the stresses, this defines a sequence of lifted surfaces, all of which have negative discrete curvature at every vertex except for a single maximum vertex.

Does this process converge to some limit? What can be said about the limiting surface? Are there combinatorial conditions on the sequence of frameworks that ensure that the limit is something like a smooth pseudo-sphere?

One could ask the same question with a different model of generating “random” Laman circuits. For example, the PPT-polytope of [19] is a polytope whose vertices are in one-to-one correspondence with the pointed pseudo-triangulations on a given point set. Choosing an extreme vertex in a random direction (for a randomly generated point set) produced a pseudo-triangulation, to which we can add an edge to create a “random” Laman circuit. Limit shapes like this have appeared in other contexts, for example for random convex polygons [3], [4].

The results in Section 4 interpreted necessary conditions in Section 2 on the self-stress at the vertices and faces of the original non-crossing framework as necessary conditions on the lifting. It is natural to reverse this idea by starting from a piecewise-linear surface and projecting it back to the plane.

**Open Problem 6.** Characterize geometrically exactly which piecewise-linear spatial surfaces, projecting one to one onto the entire plane, project to planar frameworks with non-crossing reciprocals.

### 5.5. *Non-Crossing Reciprocals with Respect to Other Embeddings*

If a graph admits several topologically different embeddings in the plane, one may decide to construct the reciprocal of a non-crossing framework on that graph taking as face and vertex cycles those of a different plane embedding from the one given by the framework. Alternatively one may not allow this but decide to call the reciprocal non-crossing if it is non-crossing as a geometric graph, even if its face structure is not dual to the one in the original.

Our characterizations of non-crossing reciprocal pairs do not address these situations. Note that this is only an issue for non-3-connected graphs, and that graphs with cut vertices need not be considered: every self-stress can be decomposed as a sum of self-stresses supported in 2-connected components.

There are two questions that should be addressed here.

**Open Problem 7.** Is there a non-crossing framework  $G$  (necessarily 2-connected but not 3-connected) whose natural reciprocal has no crossing edges but is embedded differently from the graph-theoretic planar dual of  $G$ ?

We know that this cannot happen when  $G$  is a Laman circuit (see Theorem 7), but for frameworks with more edges, the question is open.

**Open Problem 8.** Characterize pairs of non-crossing frameworks which are reciprocals to one another, but not necessarily with respect to the face and vertex cycles given by their embeddings as frameworks.

### 5.6. *What Planar Graphs Produce Non-Crossing Reciprocal Pairs?*

We finish with perhaps the broadest question of all:



**Open Problem 9.** Given a 2-rigid planar graph, decide (give a characterization, or at least a reasonable algorithm) whether it has a non-crossing generic embedding with a good self-stress.

We know for example that for all Laman circuits such an embedding exists: any generic pseudo-triangulation embedding works. In order for a generic framework to have a self-stress on all edges, it must be 2-rigid—remain rigid after deletion of any one edge [14]. However, we also know that not all planar 2-rigid graphs have such an embedding (Fig. 14).

### Acknowledgments

This research was initiated at the Workshop on Rigidity Theory and Scene Analysis organized by Ileana Streinu at the Bellairs Research Institute of McGill University in Barbados, Jan. 11–18, 2002 and partially supported by NSF Grant CCR-0203224.

### References

1. O. Aichholzer, F. Aurenhammer, P. Braß, and H. Krasser, Spatial embeddings of pseudo-triangulations, *Proc. 19th Ann. Symp. Comput. Geom.*, 2003, pp. 144–153.
2. P. Ash, E. Bolker, H. Crapo, and W. Whiteley, Convex polyhedra, Dirichlet tessellations, and spider webs, in *Shaping Space: A Polyhedral Approach* (M. Senechal and G. Fleck, eds.), Birkhäuser, Boston, MA, 1988, pp. 231–250.
3. I. Bárány, The limit shape of convex lattice polygons, *Discrete Comput. Geom.* **13** (1995), 270–295.
4. I. Bárány, G. Rote, W. Steiger, and C.-H. Zhang, A central limit theorem for convex chains in the square, *Discrete Comput. Geom.* **23** (2000), 35–50.
5. R. Bow, *Economics of Construction in Relation to Framed Structures*, E. and F. N. Spon, London, 1873.
6. H. Crapo and W. Whiteley, Plane self stresses and projected polyhedra, I: the basic pattern, *Structural Topology* **20** (1993), 55–78.
7. H. Crapo and W. Whiteley, Spaces of stresses, projections and parallel drawings for spherical polyhedra, *Beiträge Algebra Geom.* **35**(2) (1994), 259–281.
8. L. Cremona, *Le Figure Reciproche Nella Statica Grafica*, Milano, 1872. English translation: *Graphical Statics*, Oxford University Press, Oxford, 1890.
9. C. Culmann, *Die graphische Statik*, Meyer und Zeller, Zürich, 1866.
10. J. Graver, B. Servatius, and H. Servatius, *Combinatorial Rigidity*, Graduate Studies in Mathematics, vol. 2, American Mathematical Society, Providence, RI, 1993.
11. R. Haas, D. Orden, G. Rote, F. Santos, B. Servatius, H. Servatius, D. Souvaine, I. Streinu, and W. Whiteley, Planar minimally rigid graphs and pseudo-triangulations, *Proc. 19th Ann. Symp. Comput. Geom.*, 2003, pp. 154–163. Full version (preprint July 2003, 25 pages) available at <http://arxiv.org/abs/math.CO/0307347>.
12. D. A. Huffman, Impossible objects as nonsense sentences, in *Machine Intelligence*, Vol. 6 (B. Meltzer and D. Michie, eds.), Edinburgh University Press, Edinburgh, 1971, pp. 295–323.
13. D. A. Huffman, A duality concept for the analysis of polyhedral scenes, in *Machine Intelligence*, Vol. 8 (E. W. Elcock and D. Michie, eds.), Wiley, New York, 1977, pp. 475–492.
14. B. Jackson and T. Jordán, Connected rigidity matroids and unique realizations of graphs, Technical Report TR-2002-12, Egerváry Research Group on Combinatorial Optimization, Budapest, 2002. [www.cs.elte.hu/egres](http://www.cs.elte.hu/egres).
15. G. Laman, On graphs and rigidity of plane skeletal structures, *J. Engrg. Math.* **4** (1970), 331–340.
16. J. C. Maxwell, On reciprocal figures and diagrams of forces, *Philos. Mag.* **4**(27) (1864), 250–261.

17. D. Orden, F. Santos, B. Servatius, and H. Servatius, Combinatorial pseudo-triangulations, preprint, July 2003. <http://arxiv.org/abs/math.CO/0307370>.
18. D. Orden and F. Santos, The polytope of non-crossing graphs on a planar point set, preprint, February 2003. <http://arxiv.org/abs/math.co/0302126>.
19. G. Rote, F. Santos, and I. Streinu, Expansive motions and the polytope of pointed pseudo-triangulations, in *Discrete and Computational Geometry—The Goodman–Pollack Festschrift* (B. Aronov, S. Basu, J. Pach, and M. Sharir, eds.), Algorithms and Combinatorics, Vol. 25, Springer-Verlag, Berlin, 2003, pp. 699–736. [arxiv.org/abs/math.CO/0206027](http://arxiv.org/abs/math.CO/0206027).
20. G. Rote, C. A. Wang, L. Wang, and Y. Xu, On constrained minimum pseudotriangulations, in *Computing and Combinatorics*, Proc. 9th Internat. Comput. Combin. Conf. (COCOON 2003), July 2003 (T. Warnow and B. Zhu, eds.), Lecture Notes in Computer Science, Springer-Verlag, Berlin, 2003. <http://page.inf.fu-berlin.de/~rote/Papers/abstract/On+constrained+minimum+pseudotriangulations.html>.
21. B. Roth and W. Whiteley, Tensegrity frameworks, *Trans. Amer. Math. Soc.* **177** (1981), 419–446.
22. E. Steinitz, Polyeder und Raumeinteilungen, in *Encyklopädie der mathematischen Wissenschaften*, Vol. 3, part 3AB12 (W. F. Meyer and H. Mohrmann, eds.), Teubner, Leipzig, 1922, pp. 1–139.
23. I. Streinu, A combinatorial approach to planar non-colliding robot arm motion planning, *Proc. 41st Symp. Found. Comput. Sci. (FOCS)*, Redondo Beach, California (2000), pp. 443–453.
24. W. T. Tutte, How to draw a graph, *Proc. London Math. Soc.* **13** (1963), 743–768.
25. N. White and W. Whiteley, The algebraic geometry of stress in frameworks, *SIAM J. Algebraic Discrete Methods* **4** (1983), 481–511.
26. W. Whiteley, Motions and stresses of projected polyhedra, *Structural Topology* **7** (1982), 13–38.
27. W. Whiteley, Matroids and rigid structures, in *Matroid Applications* (N. White, ed.), Cambridge University Press, Cambridge, 1992, pp. 1–53.

Received September 8, 2003, and in revised form April 5, 2004. Online publication August 19, 2004.